Spontaneous ferromagnetic spin ordering at the surface of La_2CuO_4

R. V. Yusupov,[1,*] V. V. Kabanov,[1] D. Mihailovic,[1,2] K. Conder,[3] K. A. Müller,[4] and H. Keller[4]
[1]*Jozef Stefan Institute, Jamova 39, 1000 Ljubljana, Slovenia*
[2]*University of Ljubljana, Jadranska 19, 1000 Ljubljana, Slovenia*
[3]*Laboratory for Neutron Scattering, ETH Zürich and PSI, CH-5232 Villigen PSI, Switzerland*
[4]*Physik-Institut der Universität Zürich, Winterthurerstrasse 190, CH-8057, Switzerland*
(Received 9 March 2007; revised manuscript received 31 May 2007; published 23 July 2007)

Magnetic properties of high purity stoichiometric La_2CuO_4 nanoparticles are systematically investigated as a function of particle size. Ferromagnetic single-domain spin clusters are shown to spontaneously form at the surface of fine grains as well as paramagnetic defects. Hysteresis loops and thermomagnetic irreversibility are observed in a wide temperature range 5–350 K with the remnant moment and coercivity gradually decreasing with increasing temperature. Possible origins of the spontaneous surface ferromagnetic clusters and the relation of our data to the appearance of unusual magnetic phenomena and phase separation of doped cuprates are discussed.

DOI: 10.1103/PhysRevB.76.024428 PACS number(s): 75.70.Rf, 75.50.Tt, 75.50.Ee, 74.25.Ha

I. INTRODUCTION

High-temperature superconductors (HTSCs) have been investigated for more than twenty years but still new important details of their physical structure and properties are being discovered. Moreover, in spite of the clear progress achieved in the clarification of the phase diagram of cuprates, the spin dynamics in relation to superconductivity in these compounds remains unclear.

One of the things which is no doubt of crucial importance in undoped and lightly doped cuprates is magnetism and magnetic (exchange) interactions. This is clear from the simple observation that the magnetic order in La_2CuO_4 is strongly influenced by the non-stoichiometry or chemical doping needed for the superconductivity to arise (see, e.g., Ref. 1). Thus, the parent La_2CuO_4 has the Néel temperature T_N=325 K. For $La_{2-x}Sr_xCuO_4$ T_N decreases sharply with the increase of Sr doping. In the case of La_2CuO_{4+y} the situation is even more peculiar. The compound within the so-called miscibility gap (1–6 % of excess oxygen) tends to phase separate into the superconducting (below ~40 K) oxygen-rich and nearly stoichiometric oxygen-poor regions. The sample is found to be macroscopically inhomogeneous, and the Néel temperature for the oxygen-poor phase is $T_N \approx 260$ K being the characteristic one in the above rather wide range of the excess oxygen concentrations. It looks clear that in the case of Sr-doped La_2CuO_4 the local inhomogeneity due to impurity disorder and structural twinning is also the intrinsic property of the material.

The unusual magnetic properties of the fine grains and nanoparticles of the antiferromagnetic (AF) in the bulk transition metal oxides were predicted by Néel[2] to arise from the uncompensated magnetic moments of the same sublattice found at the grain surface. Such magnetism was really observed and attracted the attention of the researchers due to its practical use. During the last decades the results on NiO,[3–7] MnO,[8] Cr_2O_3,[4] CoO,[9–11] Fe_2O_3,[4] CuO,[12] and ferritin[13–15] have been published. Large magnetic moments were found and phenomena peculiar, especially for antiferromagnets were observed, such as superparamagnetism and exchange bias.

In this paper we present the results of the detailed magnetic studies of stoichiometric La_2CuO_4 fine grains. The compound has a layered perovskite crystal structure and its magnetic structure is more complicated than the structures of binary transition metal oxides. It is almost ideal two-dimensional (2D) Heisenberg antiferromagnet with the strong superexchange in the CuO_2 planes. Spin canting due to Dzyaloshinskii-Moriya interaction below the structural phase transition at ~530 K produces a nonzero out-of-plane magnetic moment for each CuO_2 plane. These moments order antiferromagnetically at T_N=325 K. The interaction of the moments with an applied magnetic field can overcome the interplane exchange interaction and lead to the so-called weak ferromagnetism.[16]

We have found an unusual relatively strong nonlinear component in its magnetization as a function of applied field characteristic of anisotropic ferromagnetic single-domain particles. It is shown that this magnetism arises from the surface of the material, but is not due to uncompensated surface moments proposed by Néel. Grain boundaries are known as one of the limiting factors for practical applications of HTSC materials and the surface phenomenon described here may be important from this point of view. Some of the hysteretic behavior of the magnetization reported for cuprates in a number of works[17–22] may be of similar origin to that which we observe.

II. EXPERIMENTAL PROCEDURE

The polycrystalline samples of La_2CuO_4 were prepared by a solid-state reaction using La_2O_3 and CuO of a minimum purity of 99.99%. The respective amounts of the starting reagents were mixed and then calcinated at 950–1150 °C for 80 h in air, with several intermediate grindings. Phase purity of the sample was checked with x-ray diffractometer (SIEMENS D500).

The as-grown samples were found to be slightly oxygen-enriched having $T_N \approx 260$ K and containing a very small amount of superconducting inclusions with $T_c \approx 30$ K and Meissner phase volume fraction of about 4×10^{-4}. After

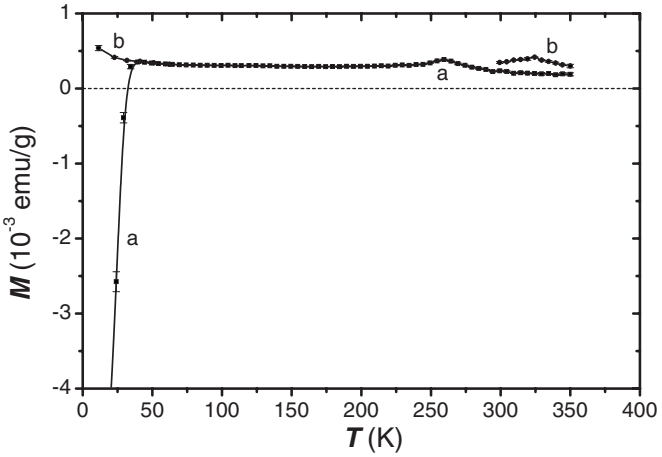

FIG. 1. Temperature dependence of the magnetization of the as-grown (a) and annealed in argon (b) La_2CuO_4 polycrystalline samples before grinding, $H_{meas}=1000$ Oe.

annealing at 600 °C for 2 h in a flow of pure Ar (~99.999%) the sample had $T_N=325$ K and no detectable diamagnetic inclusions. In Fig. 1 the temperature dependence of the magnetization of the sample before and after the annealing in the measuring field of 1000 Oe is shown.

In order to obtain a series of samples with different average grain size, the annealed compound was ground for 8 h in an agate mortar in dry high-purity isopropanol. The ground samples were dispersed by ultrasound and the grains of different sizes were extracted by means of successive sedimentation and further characterized with scanning electron (SEM) and atomic force (AFM) microscopes. Obtained grain size histograms were well described with the log-normal distribution. The samples had the grain size mean values of 0.22, 0.68, 1.53, and 4.1 μm and the masses were 22, 36, 64, and 35 mg, respectively. The SEM image of the 0.68 μm sample is shown in Fig. 2. X-ray diffraction patterns have shown that all the samples in the series are crystalline and single-phase. It is worth noting here that La_2CuO_4 compound is stable in air and in water [unlike other cuprates such as $YBa_2Cu_3O_{6+y}$ or Sr_2CuO_3 (Ref. 23)].

The magnetic measurements were performed with a commercial Quantum Design MPMS-5 superconducting quantum interference device (SQUID) magnetometer. The samples were put into the gelatin capsules and mounted in a

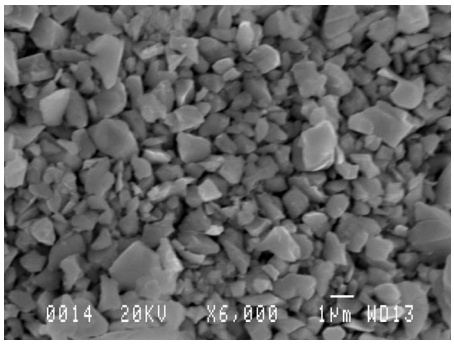

FIG. 2. SEM image of the La_2CuO_4 sample with the average grain size of 0.68 μm.

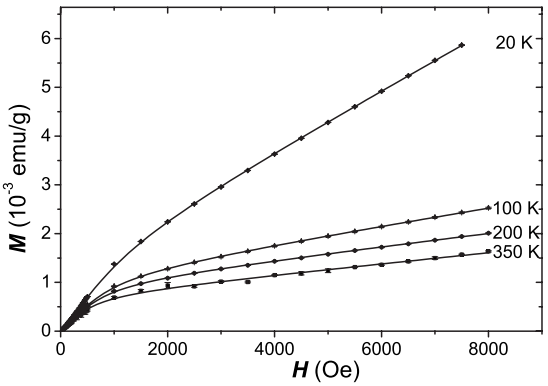

FIG. 3. Temperature variation of the magnetization curve of the 1.53 μm La_2CuO_4 sample. The lines are the fits with Eq. (1).

polypropylene drinking straw. In order to avoid the distortion of the $M(H)$ curves due to the observed memory effects, the "no overshoot" mode for target field approach was used. Scan length was 4 cm with 24 points per scan. At each point the average over five measurements was taken as a result. The characteristic measurement time is $\sim 10^2$ s.

III. EXPERIMENTAL RESULTS

The magnetization curves of the sample with the average grain size of $\langle d \rangle \approx 1.53$ μm for different temperatures are shown in Fig. 3. In Fig. 4 the observed at $T=200$ K curves for different samples are shown. It is clearly seen that these dependencies consist of two main contributions: a nonlinear ferromagnetic one, saturating at $H \sim 4000$ Oe, and a linear one. The magnetization curves can thus be described as

$$M(H) = \chi H + M_{nl}(H). \quad (1)$$

The nonlinear component $M_{nl}(H)$ at all the temperatures can be reasonably well described by the Brillouin (Langevin) function used for the paramagnetic (superparamagnetic) objects. The fit with the Brillouin function describing $M_{nl}(H)$ (Fig. 3) gives the temperature-dependent cluster spin values 11 000±500, 5000±300, 2000±200, and 300±20 at 350,

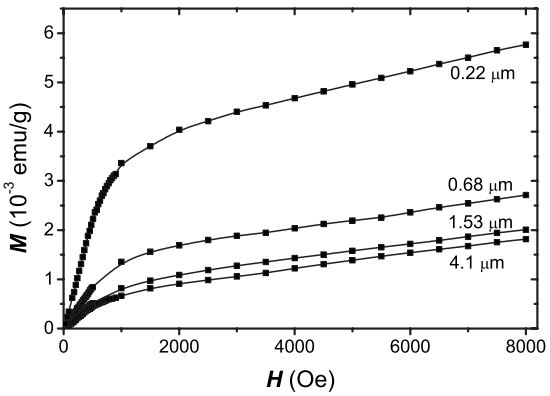

FIG. 4. Magnetization curves of La_2CuO_4 fine particle samples for different average grain sizes, $T=200$ K. The lines are guides for the eye.

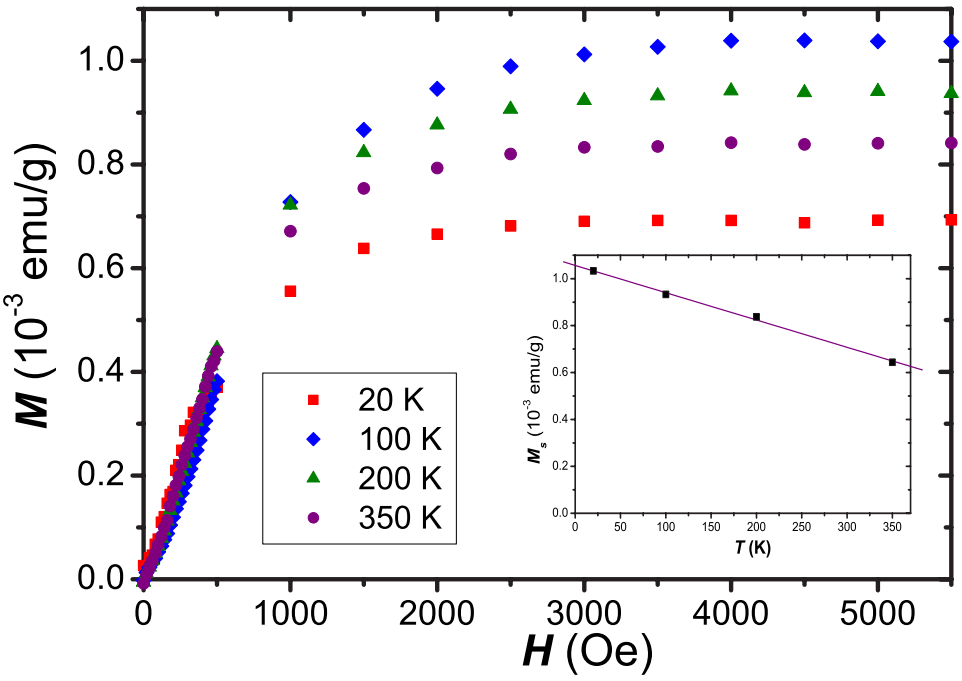

FIG. 5. (Color online) Temperature variation of the nonlinear magnetization component of 1.53 μm La_2CuO_4 sample. In the inset the temperature dependence of the nonlinear saturated magnetic moment is shown.

200, 100, and 20 K, respectively. The $M(H)$ dependencies for all the samples were found to be the same, differing only in magnitude of the linear and the nonlinear terms. The total spin values characterizing the nonlinear component within the fit error did not reveal any grain size dependence.

In Fig. 5 the nonlinear magnetization component $M_{nl}(H)$ obtained by the subtraction of the linear term is shown for a set of temperature values. This plot indicates that we are not dealing with the usual superparamagnetic behavior, otherwise the initial slope of these curves should depend on T.

In the inset of Fig. 5 the temperature dependence of the saturated magnetic moment is shown. In the temperature range 20–350 K it has a nearly linear character.

In order to determine if the unusual magnetism of our samples comes from the bulk or the surface, a grain size dependence of the magnetization has been studied. In Fig. 6 these data for the nonlinear magnetization components at several temperatures are presented. It is characterized by the saturated magnetic moment M_s.

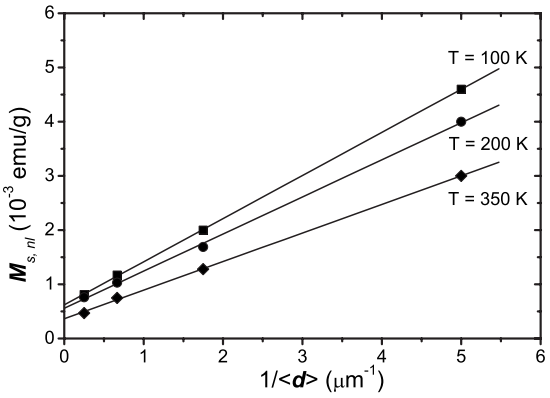

FIG. 6. Grain size dependence of the saturated nonlinear magnetization component moment.

The magnetic susceptibility describing the linear magnetization component is found to be significantly greater than the susceptibility of bulk stoichiometric La_2CuO_4.[24] Grain size dependence of the excess susceptibility with respect to the bulk La_2CuO_4 $\chi_e=\chi-\chi_B$ at $T=20$ K is shown in Fig. 7 (this term is strongly pronounced at low temperatures). The values of χ_B for the bulk material were taken from the data of Lavrov *et al.*[24] as the orientational averages $\chi_B=(\chi_a+\chi_b+\chi_c)/3$ [e.g., at $T=20$ K $\chi_B=1.81\times10^{-7}$ emu/(g Oe)].

The clear linear dependences of both M_s and χ_e on $1/\langle d\rangle$, which is the surface to volume ratio, allow us to assign unambiguously both components of $M(H)$ to the grain surface. The Curie-like $1/T$ dependence of χ_e shown in the inset of Fig. 7 reveals a paramagnetic character of this linear magnetization term.

To investigate the origin of the different components, we annealed the 0.68 μm sample after the grinding procedure in the same way (2 h at 600 °C in the flow of Ar) as it was annealed initially. It had led to almost total, more than 80%, removal of the excess Curie-like component. The nonlinear ferromagnetic component was reduced much less, only by ~30%, indicating that unlike the linear Curie-like term the latter is rather stable with respect to annealing.

The explanation of the Curie-like magnetization component now looks more straightforward. It most probably originates from the surface Cu^{2+} paramagnetic defects that have been observed in EPR spectra of La_2CuO_{4+y} fine powders and ceramics and described by Wübbeler *et al.*[25] So, in the remainder of the paper we will be mainly interested in the properties of the nonlinear magnetization component.

The measured zero-field cooled (ZFC) and field cooled (FC) in the field of 10 kOe $M(T)$ dependencies are shown in Fig. 8. Thermomagnetic irreversibility is found in the whole measured temperature range 5–300 K and no characteristic spike corresponding to the blocking temperature is found neither in FC nor in ZFC curves.

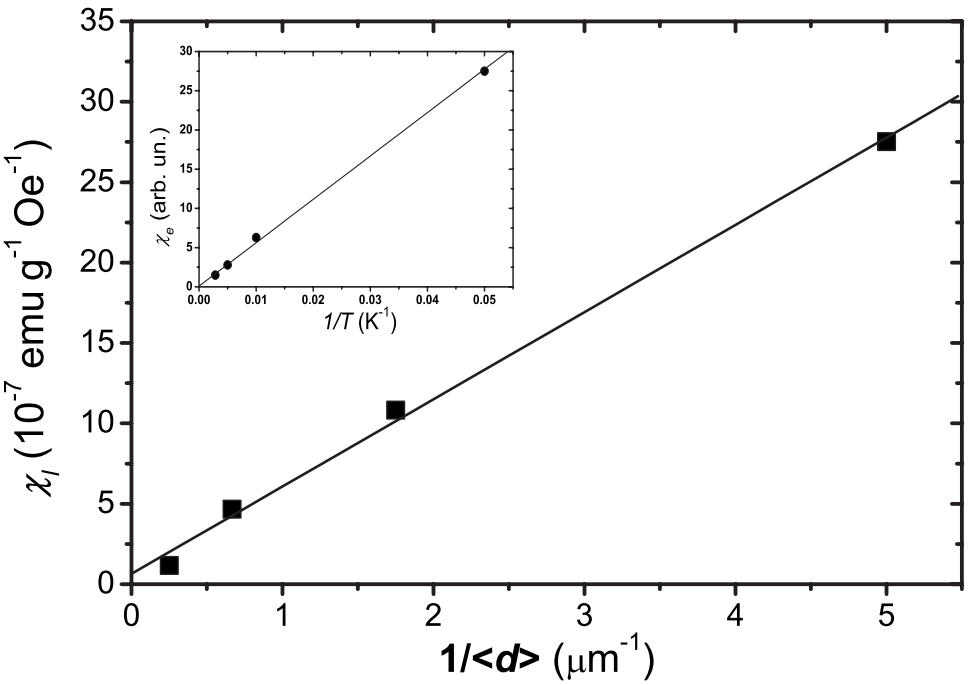

FIG. 7. Grain size dependence of the excess in respect to the bulk value susceptibility χ_e describing the linear magnetization component. In the inset the temperature dependence of χ_e is shown for 0.22 μm La_2CuO_4 sample.

Hysteresis loops are observed at all temperatures up to 350 K (Fig. 9). This hysteresis obviously corresponds to the nonlinear magnetization term. At $T=100$ K the loop is open up to 2000 Oe. With increasing temperature the hysteresis loop closes in the gradually decreasing field. This is demonstrated also by the smoothly decreasing difference between FC and ZFC curves in Fig. 8.

The hysteresis loop is symmetric either for FC or for ZFC samples at any temperature. This means that no detectable exchange bias arising usually at the boundary of ferromagnetically and antiferromagnetically ordered phases takes place.

The remnant magnetization relaxes rather slowly. The magnetization decay is shown in Fig. 10. The decay is described well by the equation $M(t)=M_0(1-S\ln t)$, where M_0 is the initial magnetization after the removal of the applied magnetic field and S is the magnetic viscosity.

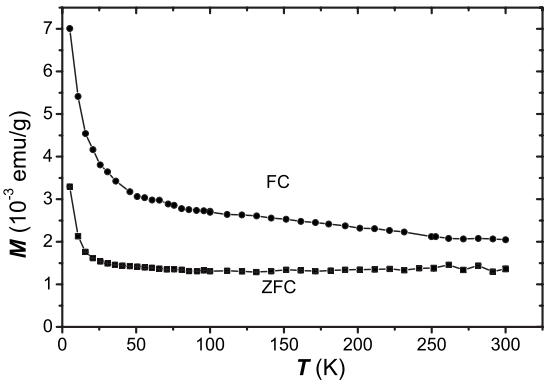

FIG. 8. Temperature dependencies of magnetization of zero-field cooled (ZFC) and field-cooled (FC) in the field of 10 kOe for 0.22 μm La_2CuO_4 sample.

A puzzling fact at the first sight is that no characteristic spike in the $M(T)$ curve corresponding to 3D AF ordering as in Fig. 1 was observed for the 0.22 μm grain size sample (the data is not shown). In our opinion, this is simply because the surface magnetization dominated over the bulk one and the dynamic range of the magnetometer was insufficient to reveal this feature. Indeed, the spike amplitude for the initial sample in the field of 1000 Oe is $\sim 10^{-4}$ emu/g while the magnetization of the sample with the grain size 0.22 μm in this field is $\sim 2.4\times 10^{-3}$ emu/g. The spike thus should be $\sim 4\%$ of the signal, and taking into account that the sample mass was only 22 mg, this value could be difficult to detect.

IV. DISCUSSION

The first question we are going to discuss is whether the observed magnetization properties are intrinsic for La_2CuO_4.

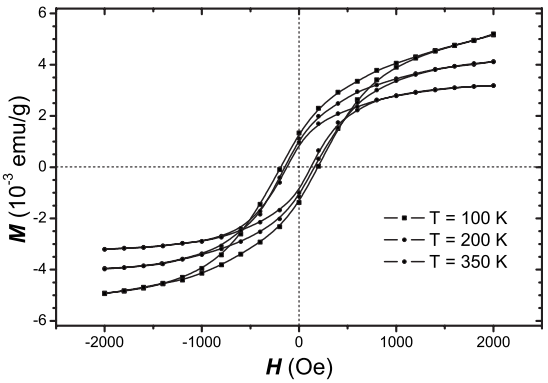

FIG. 9. Magnetization hysteresis loop and its temperature variation for 0.22 μm La_2CuO_4 sample.

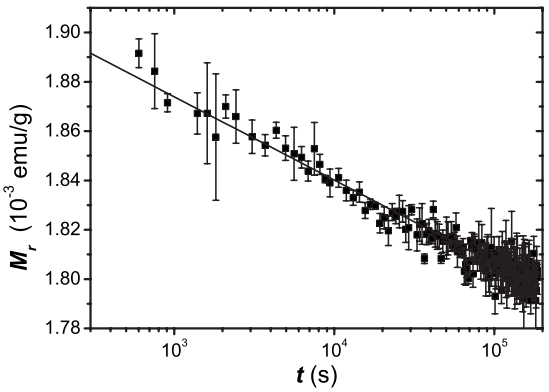

FIG. 10. Decay of the remnant magnetization moment of the 0.22 μm sample at $T=30$ K.

In our opinion, usage of high-purity initial components and solvents during the sample processing allows us to eliminate the possibility of chemical contamination of the sample. Another possible reason would be a formation of $Cu(OH)_2$ compound at the surface of the grains exposed to the air, where the highly reactive broken bonds occur (as it was mentioned already, La_2CuO_4 itself is stable in air and water). Nevertheless, this compound is not ferromagnetic, so its formation definitely cannot explain our observations. Also, very similar magnetic properties were found for CuO (Ref. 12) and MnO (Ref. 6) nanoparticles that were synthesized in a totally different way than in our case. Another argument for an intrinsic origin of our magnetization is that qualitatively similar rather weak thermomagnetic irreversibility and hysteresis loops were found even for high-quality single crystals of $La_{2-x}Sr_xCuO_4$,[21,22] the possible connection of which to our data will be discussed later.

Our results can be understood well in the following way. The observation of the hysteresis loops and irreversibility even for the smallest particles of 0.22 μm in size in the whole temperature range 5 –350 K unambiguously shows that anisotropic ferromagnetic clusters are formed at the grain's surface. The fit of the nonlinear magnetization component with the Brillouin function with the total spin values independent on the grain size within 0.2–4 μm range clearly manifests that the average magnetic cluster size is geometrically significantly smaller than the characteristic size of the particles. The fit with the Brillouin function should be nevertheless treated as formal, not revealing any physical quantities, but demonstrating the universal evolution of the $M(H)$ dependencies with temperature.

In order to explain the details of our observations let us consider the model describing the magnetization of an ensemble of single-domain anisotropic ferromagnetic particles (Fig. 11). We assume here that local field is equal to the external field, implying a low concentration of FM particles. The potential energy of such a particle in a magnetic field is a sum of the magnetic anisotropy energy and the energy of interaction of the particle's magnetic moment with the applied field

$$U = KV\sin^2\theta - \mu \cdot \mathbf{H}, \tag{2}$$

where K is the magnetic anisotropy constant, V is the volume of the particle, $\mu=M_sV$ is the particle magnetic moment, M_s is the particle saturated magnetization, $\mathbf{H}$ is the applied magnetic field, and θ is the angle between the particle easy axis and its magnetic moment. There are two limiting and physically distinct cases: with the magnetic field applied along and perpendicular to its easy axis.

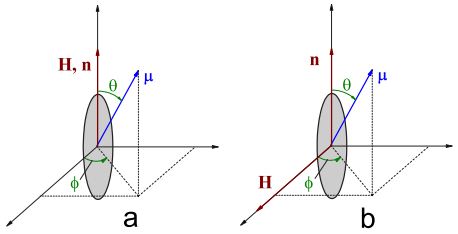

FIG. 11. (Color online) The sketches used in the calculations of the ferromagnetic particle energy for the cases of (a) $\mathbf{H}\|\mathbf{n}$ and (b) $\mathbf{H}\perp\mathbf{n}$.

In the case of $\mathbf{H}\|\mathbf{n}$, where $\mathbf{n}$ is a unit vector describing the orientation of the particle easy axis [Fig. 11(a)], the energy of a particle is

$$U = KV\sin^2\theta - \mu H\cos\theta. \tag{3}$$

It can be rewritten introducing the effective anisotropy field $H_a=2K/M_s$ and dimensionless field $h=H/H_a=HM_s/2K$ as

$$U = \mu H_a\left(\frac{\sin^2\theta}{2} - h\cos\theta\right). \tag{4}$$

Similarly, for $\mathbf{H}\perp\mathbf{n}$ [Fig. 11(b)], energy of a particle is described by the expression

$$U = \mu H_a\left(\frac{\sin^2\theta}{2} - h\sin\theta\cos\phi\right). \tag{5}$$

Note that in both cases for the given values of macroscopic parameters K and M_s the energy landscape amplitude scales with a particle volume V with the product $\mu H_a=KV$ serving as scaling factor, while its pattern is defined by the ratio $h=H/H_a$. The potential energy patterns for these characteristic cases are shown in Figs. 12 and 13.

In both cases two minima separated by the energy barrier are present, depending on h. For $h=1$ only a single minimum

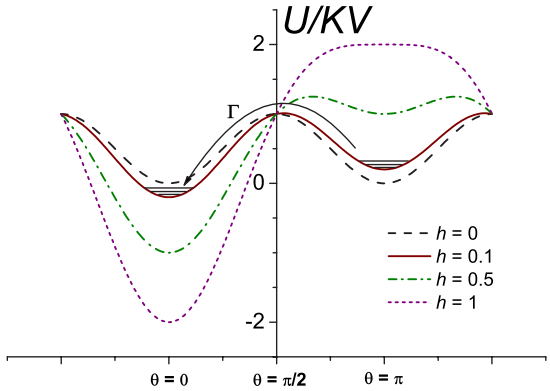

FIG. 12. (Color online) Potential energy cross sections $U(\theta,\phi)$ for the case of $\mathbf{H}\|\mathbf{n}$ with $\phi=0$ and different values of applied field $h=H/H_a$.

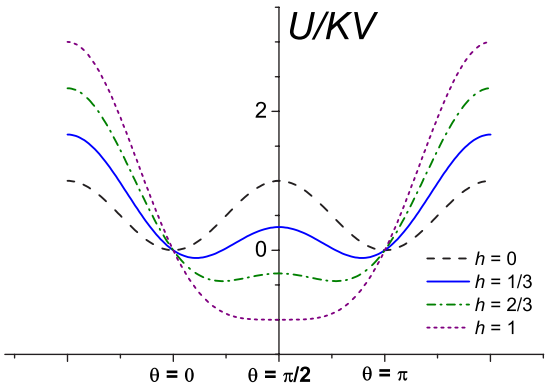

FIG. 13. (Color online) Potential energy cross sections $U(\theta,\phi)$ for the case $\mathbf{H}\perp\mathbf{n}$ with $\phi=0$ and different values of applied field $h=H/H_a$.

remains. The principal difference is that with $\mathbf{H}\perp\mathbf{n}$ energies in the minima are equal, while with $\mathbf{H}\|\mathbf{n}$ the minima are inequivalent. In the former case the system is in equilibrium with any applied field. In the latter case the situation is different, and the relaxation towards equilibrium is prevented by the small probability to overcome the barrier.

Magnetization of the collection of identical particles for these two cases can be easily treated assuming $k_BT \ll \mu H_a$. So, for particles with $\mathbf{n}\perp\mathbf{H}$ magnetization takes place due to the shift of the energy minima towards the direction of the applied field, and can reasonably well be described as [see also Fig. 14(b)]

$$\mathfrak{M}_\perp(H,T) = \begin{cases} h & \text{for } H < H_a, \\ 1 & \text{for } H \geqslant H_a, \end{cases} \tag{6}$$

where $\mathfrak{M}=M/M_0$ is a normalized magnetization and $M_0=N\mu$ is the total magnetic moment of the system. For particles with $\mathbf{n}\|\mathbf{H}$ the equilibrium magnetization $\tilde{\mathfrak{M}}$ within the same assumption can be approximated by

$$\tilde{\mathfrak{M}}_\|(H,T) = \tanh\left(h\frac{\mu H_a}{k_BT}\right) = \tanh\left(\frac{\mu H}{k_BT}\right). \tag{7}$$

In general for the parallel field the system is only partly in equilibrium due to the presence of the energy barrier. The measured magnetization would be a product of equilibrium magnetization to the fraction of the system that is in equilibrium $\eta(H,T)$:

$$\mathfrak{M}(H,T) = \tilde{\mathfrak{M}}(H,T)\,\eta(H,T). \tag{8}$$

This fraction may be easily estimated. The probability Γ to overcome the barrier is defined by the Néel-Brown equation

$$\Gamma = \tau^{-1} = \tau_0^{-1}\exp(-U_B/k_BT), \tag{9}$$

where τ is the relaxation time and $\tau_0 \sim 10^{-10}$ s is the so-called microscopic attempt time, E_B is the barrier height. The last is exactly equal to

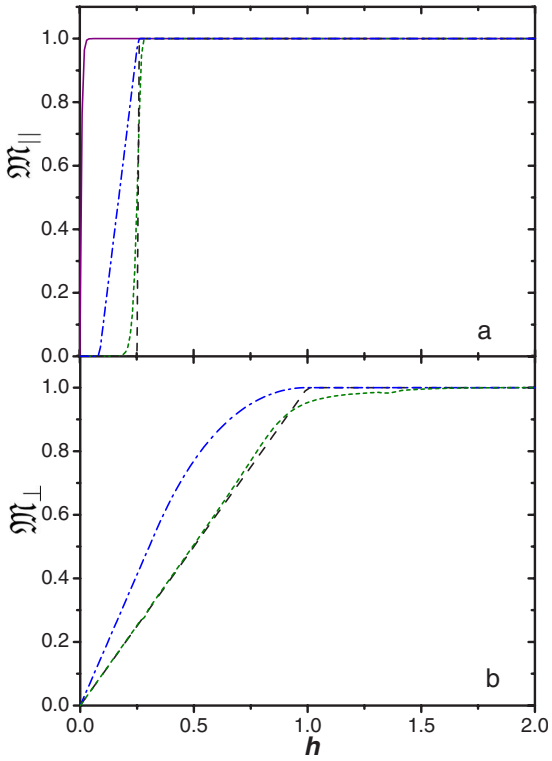

FIG. 14. (Color online) The simulated magnetization curves for the particles with (a) $\mathbf{n}\|\mathbf{H}$ and (b) $\mathbf{n}\perp\mathbf{H}$. Short-dash and dashed lines correspond to the numerical and approximate $M(H)$ curves for fixed H_a, while the dash-dot line is an average for particle collection with the distribution of H_a as described in the text (field h in this case is defined as $h=H/H_a^+$); solid line in panel (a) is an equilibrium magnetization described by Eq. (7).

$$U_B(H) = \frac{\mu H_a}{2}(1-h)^2, \tag{10}$$

and for given characteristic measurement time τ_m $\eta(H,T)$ is equal to

$$\eta(H,T) = \frac{1}{\tau_m}\int_0^{\tau_m} e^{-t/\tau}dt = 1 - e^{-\tau_m/\tau}. \tag{11}$$

If $\tau \ll \tau_m$ at any field, magnetization of such particle collection will be reversible, and this is the case of superparamagnetism. In the opposite case, the system is locked in energy minima until one is destroyed by applied field. Magnetization of a system then will be irreversible, and this is the case of ferromagnetism.

The magnetization curves in the conditions of $\mu H_a/k_BT=0.01$, $\tau_m=100$ s^{-1}, and $\tau_0=10^{-10}$ s^{-1} with the easy axes parallel and perpendicular to the applied field are shown in Figs. 14(a) and 14(b), respectively.

It is readily seen that $\mathfrak{M}(H)$ curve for the particles with $\mathbf{n}\|\mathbf{H}$ in the limit of $k_BT \ll \mu H_a$ can well be approximated by the theta function

$$\mathfrak{M}_\|(H) = \begin{cases} 0 & \text{for } h < h_c, \\ 1 & \text{for } h \geqslant h_c, \end{cases} \tag{12}$$

where h_c is the applied magnetic field, at which $\tau=\tau_m$. As follows from Eqs. (9) and (10)

$$h_c = 1 - \sqrt{\frac{2k_BT}{\mu H_a} \ln \frac{\tau_m}{\tau_0}}. \tag{13}$$

To make our treatment more realistic we introduce the distribution of the anisotropy fields $f(H_a)$ in the simplest flat form within the values H_a^- to H_a^+, leaving other parameters (K,V,μ) constant:

$$f(H_a) = \begin{cases} \dfrac{1}{H_a^+ - H_a^-} & \text{for } H_a^- \leqslant H_a \leqslant H_a^+, \\ 0 & \text{for } H_a < H_a^- \text{ and } H_a > H_a^+. \end{cases} \tag{14}$$

From here on there is no sense in using dimensionless field h, so the real one H will be used. For the particles with $\mathbf{n} \perp \mathbf{H}$ the situation can be treated analytically:

$$\mathfrak{M}_\perp(H) = \begin{cases} \dfrac{H}{H_a^+ - H_a^-} \ln \dfrac{H_a^+}{H_a^-} & \text{for } H \leqslant H_a^-, \\ \dfrac{H - H_a^- + H \ln(H_a^+/H)}{H_a^+ - H_a^-} & \text{for } H_a^- < H < H_a^+, \\ 1 & \text{for } H \geqslant H_a^+. \end{cases} \tag{15}$$

At the initial stage the $\mathfrak{M}_\perp(H)$ curve is linear with an effective susceptibility defined by the distribution of H_a. With $H > H_a^-$, the fraction of the system saturates, and effective slope becomes dependent on H, until magnetization is totally saturated at $H \geqslant H_a^+$. Note, that still for these particles magnetization process is totally reversible. The $\mathfrak{M}_\perp(H)$ curve for this case with H_a^+ and H_a^- defined by $\mu H_a^+/k_BT=300$ and $\mu H_a^-/k_BT=100$ is shown in Fig. 14.

For the particles with $\mathbf{n} \| \mathbf{H}$ the situation can well be approximated if we assume that for all the particles, similar to the situation described by Eq. (12), the equilibrium magnetization is saturated at $h > h_c$, which is again valid for $k_BT \ll \mu H_a$. Thus, we have simply to average theta-function on the distribution $f(H_a)$. The result is

$$\mathfrak{M}_\parallel(H) = \begin{cases} 0 & \text{for } \tilde{H} < H_a^-, \\ \dfrac{\tilde{H} - H_a^-}{H_a^+ - H_a^-} & \text{for } H_a^- < \tilde{H} < H_a^+, \\ 1 & \text{for } \tilde{H} \geqslant H_a^+, \end{cases} \tag{16}$$

where

$$\tilde{H} = \frac{H}{1 - \sqrt{\dfrac{k_BT}{KV} \ln \dfrac{\tau_m}{\tau_0}}}. \tag{17}$$

In this situation $\mathfrak{M}_\parallel(H)$ curve reproduces the dynamics of energy barrier destruction by an applied magnetic field and thus the derivative $d\mathfrak{M}_\parallel/dH$ reflects the distribution $f(H_a)$ with the renormalized H_a scale. Note that in this case the magnetization is essentially irreversible. We should note also that in the real system not only H_a values are distributed but also particle sizes V, magnetic moments μ and orientations. Field derivative dM_{irr}/dH would reproduce the distribution of effective critical fields.

Thus, in the limit of $k_BT \ll \mu H_a$ the magnetization of both particles with $\mathbf{n} \| \mathbf{H}$ and $\mathbf{n} \perp \mathbf{H}$, only weakly depends on temperature due to a small temperature dependent term in the denominator of Eq. (17). This explains the minor variation of the field dependence of magnetization in a wide temperature range 20–350 K (Fig. 5). Field renormalization described by Eq. (17) explains well the gradual decrease of the remnant moment and coercivity with the temperature increase (Fig. 9).

As far as the magnetization relaxation is concerned, it is clear that the remnant moment of the monodispersed and aligned particle collection would be exponential as the energy scale is well defined. But in a real system presence of the distribution of energy barriers, as it was shown in Ref. 26, results in time-logarithmic decay. It reflects the situation where at any time of observation t, metastable states that are currently decaying, have the lifetime $\tau \approx t$. This is exactly what we see in Fig. 10.

Turning to the experimental results, we should note that our object, which is a collection of ferromagnetic clusters located at the surface of stoichiometric La_2CuO_4 grains, is rather poorly defined both in terms of the cluster size distribution as well as the values of the constants M_s and K. This limits any quantitative characterization of our sample. Nevertheless some definite conclusions can be reached. Thus we note the following:

(i) The fact that surface FM moment scales with the surface to volume ratio $(\propto 1/\langle d \rangle)$ even for the smallest $\langle d \rangle = 0.22$ μm grains (Fig. 6) shows unambiguously that the size of the clusters in a radial direction is much smaller than $\langle d \rangle/2 \approx 100$ nm, being of the order of 10 nm or less. The observation of the universal magnetization dependencies for all the grain sizes shows that cluster size distribution is rather universal. Moreover, it probably indicates that the characteristic size of a cluster is much less than the grain size for all the samples within the series. Comparing the observed saturated magnetization of the samples with the calculated magnetization arising from a surface entirely covered with a single layer of Cu^{2+} spins, we find the former to be much smaller, meaning that the clusters are either morphologically islandlike or possibly, cover the entire surface, but have a weakly FM canted AF structure. In the latter case, due to the magnetocrystalline anisotropy we still expect that there would be at least two domains on each grain, and the model which we have used is still applicable.

(ii) The observation of a hysteresis loop at $T=350$ K, which is well above $T_N=325$ K for the bulk compound shows clearly that the observed surface magnetism is beyond the Néel hypothesis and is probably not due to uncompensated outer planes of the same sublattice usually observed in binary transition metal oxide antiferromagnet fine grains. (We consider it unlikely that T_N increases on the surface by 25 K and more in grain samples.)

(iii) Assuming a homogeneous magnetization of the clusters, from the data shown in Fig. 5 we can conclude that its saturated moment M_s decreases almost linearly with temperature in the range 20–350 K. The observation of a flat

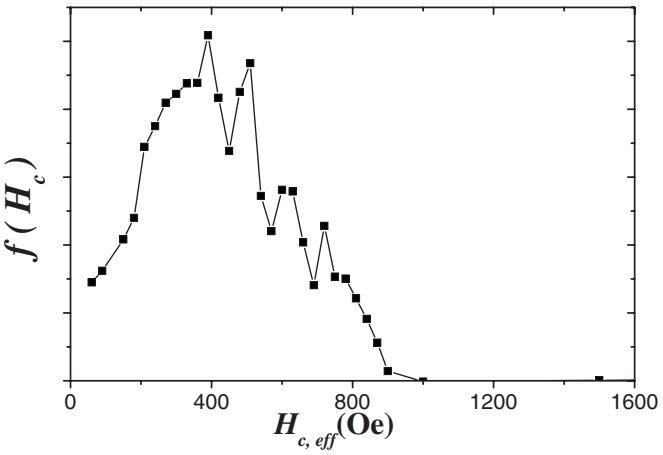

FIG. 15. Distribution of the effective critical fields obtained from the derivative of the irreversible term of magnetization curve at $T=200$ K.

ZFC $M(T)$ curve is the result of peculiar compensation of a drop of M_s with T and the growing fraction of the system in equilibrium.

(iv) The temperature-independent initial slope of the nonlinear magnetization component (Fig. 5) is determined mainly by the energy barrier destruction dynamics with the applied magnetic field. This and the hysteresis loop only slightly depending on T in the range of 5–350 K show that most of the system is in the limit $k_BT \ll \mu H_a$. Extracting the irreversible part of magnetization $M_{\text{irr}}(H)$ from a difference of a virgin $M(H)$ curve (Fig. 4) and its reversible part revealed in a hysteresis loop (Fig. 9), the distribution of the effective critical fields $f(H_{c,\text{eff}})$ can be estimated as $f(H_{c,\text{eff}}) \sim dM_{\text{irr}}/dH$, as described above (Fig. 15). Observation of the time-logarithmic decay on the time scale of 10^2–10^5 s at $T=30$ K (Fig. 10) together with the hysteresis loops up to 350 K on the time scale of 10^2 s (Fig. 9) allows us to estimate the energy barrier distribution to be within the range 0.05–1.2 eV.

Our observation of unusual surface magnetism of fine grains of bulk antiferromagnet material is not unique. As it has been mentioned earlier, similar results were found for nanoparticles of most of the antiferromagnetic transition metal binary oxides. Spontaneous surface magnetization was observed also in MnF_2 single crystal.[27,28] Close similarity can be found comparing our data to the results on CuO,[12] although the authors of Ref. 12 had not clearly assigned the ferromagnetic response of their samples to the particles surface. It looks a bit puzzling that for La_2CuO_4 fine particles we did not observe any exchange bias, as for CuO nanoparticles. This phenomenon takes place at the interface of FM and AF compounds and is usually revealed by the shift of the hysteresis loop in field by some H_E value.[29] One can suggest a number of possible reasons for this. The magnetic structure of La_2CuO_4 is more complicated than in binary oxides: it is a four-sublattice antiferromagnet with a strong anisotropy. The exchange couplings in the CuO_2 plane are much stronger than the interplane ones. The in-plane AF correlations appear at much higher temperature than $T_N=325$ K, which is a transition to 3D antiferromagnetic state. In order for the exchange bias to be observed one should cool down the sample in magnetic field through T_N, and it is a question which temperature should be defined as T_N in our case. Another, and in our opinion the simplest, reason for the absence of the exchange bias can be the fact that our particles are of much greater size than that for CuO nanoparticles in Ref. 12. Consequently, the volume of the AF core is much larger than the volume of FM shell, and thus the shell influence is not enough to stabilize the AF configuration of the core that will define after the field removal the unidirectional character of the magnetic anisotropy.

The origin of ferromagnetic response of the antiferromagnetic fine particles is a matter of current research. Néel[2] was the first who predicted such a phenomenon, but his hypothesis is not applicable in our case as it was shown above. Kodama *et al.*[7] discussed strong coercivity and hysteresis loop shifts in NiO nanoparticles to arise from the formation of multisublattice spin configurations due to broken exchange bonds of the surface sites. Another possible origin of a weak ferromagnetism at the AF grain surface is the occurrence of Dzyaloshinskii-type terms[30] of the form $\mathbf{D}\cdot[\mathbf{M}_1 \times \mathbf{M}_2]$ in the free energy of the surface layers; vector $\mathbf{D}$ is normal to the surface, $\mathbf{M}_1$ and $\mathbf{M}_2$ describe the magnetizations of AF sublattices. This kind of interaction arises due to the loss of inversion symmetry near the surface. Therefore, finite spin-orbit coupling would result in spin canting. However, La_2CuO_4 fine grains are probably not the best object to study these effects because of its relative complexity even in the bulk.[1,24]

Our results seem to be of special importance because La_2CuO_4 is a parent compound for the high-T_c superconductors. It is now commonly considered that oxygen and Sr(Ba)-doped La_2CuO_4 are strongly inhomogeneous systems. These doped compounds together with their strong tendency to twin can in principle be treated as the heterogeneous systems including the AF nearly stoichiometric grains. In this sense such a system is similar to our samples and thus the interface associated magnetism can be found.

Indeed, we mention a number of experimental observations that may be relevant to our results. Magnetic irreversibilities were observed in the works by Kremer *et al.*[17–19] in phase-separated La_2CuO_{4+y} and $La_{2-x}Sr_xCuO_4$. Hysteresis loops with the coercivity values comparable to that in Fig. 9, and thermomagnetic irreversibility were reported by Panagopoulos *et al.*[20–22] for $La_{2-x}Sr_xCuO_4$ in a wide range of Sr concentrations in polycrystalline and single crystal samples. The presence of local persistent and superparamagnetically fluctuating magnetic field was also observed by Chechersky *et al.*[31,32] by Mössbauer spectroscopy in oxygenated and deoxygenated Nd_2CuO_4 and superconducting electron-doped $Nd_{1.85}Ce_{0.15}CuO_4$ samples. The grain-boundary associated magnetism has been found by μSR technique in the $Nd_{1.85}Ce_{0.15}CuO_4$ single crystal.[33]

According to Ref. 27, in MnF_2 the surface magnetic moment arises if the dielectric constant changes significantly at the media boundary, and it even changes the moment direction for the cases of the $\varepsilon_{\text{in}} > \varepsilon_{\text{out}}$ and $\varepsilon_{\text{in}} < \varepsilon_{\text{out}}$. So, one of the possible phenomenological reasons of the observed magnetic clusters formation may be simply a modulation of the dielectric constant due to inhomogeneities like the mobile hole segregation that takes place in cuprates.

In conclusion, we have experimentally observed and characterized surface magnetic phenomena in stoichiometric La_2CuO_4 fine grains. The surface gives rise to an excess magnetization with respect to bulk material, showing both ferromagnetic and paramagnetic terms in the $M(H)$, both of which scale with the grain surface area. The paramagnetic term most probably arises from the surface Cu^{2+} defects reported earlier.[25] For the ferromagnetic component, hysteresis loops and thermomagnetic irreversibility are observed in the temperature range 5–350 K, with remnant moment and coercivity decreasing gradually with T. The observations can be well understood by assuming the formation of ferromagnetic anisotropic single-domain clusters at the grain surface. The distribution of effective critical fields is estimated. The microscopic origin of the ferromagnetic component is tentatively attributed to symmetry breaking at the sample surface, but the detailed origin is unclear at present. The spontaneous appearance of ferromagnetic islands on the surface of La_2CuO_4 might be useful in nanoscale devices for spin polarizing the electron current in multilayer spin valves. The advantage is that antiferromagnetic oxides are much more common than the ferromagnetic materials currently in use.

ACKNOWLEDGMENTS

The work was supported within the FP6, Project No. NMP4-CT-2005-517039 (CoMePhS). We thank Z. Jagličić for his help with the magnetization measurements.

*Permanent address: Kazan State University, Kremlevskaya 18, 420008 Kazan, Russia; Roman. Yusupov@ijs.si

[1] M. A. Kastner, R. J. Birgeneau, G. Shirane, and Y. Endoh, Rev. Mod. Phys. **70**, 897 (1998).
[2] L. Néel, in *Low Temperature Physics* (Gordon and Breach, New York, 1962), p. 413.
[3] J. T. Richardson and W. O. Milligan, Phys. Rev. **102**, 1289 (1956).
[4] J. Cohen, K. M. Creer, R. Pauthenet, and K. Srivastava, J. Phys. Soc. Jpn. **17**, 685 (1962).
[5] J. T. Richardson, D. I. Yiagas, B. Turk, K. Foster, and M. V. Twigg, J. Appl. Phys. **70**, 6977 (1991).
[6] S. A. Makhlouf, F. T. Parker, F. E. Spada, and A. E. Berkowitz, J. Appl. Phys. **81**, 5561 (1997).
[7] R. H. Kodama, S. A. Makhlouf, and A. E. Berkowitz, Phys. Rev. Lett. **79**, 1393 (1997).
[8] S. Sako, Y. Umemura, K. Ohshima, M. Sakai, and S. Bandow, J. Phys. Soc. Jpn. **65**, 280 (1996).
[9] C. F. J. Flipse, C. B. Rouwelaar, and F. M. F. de Groot, Eur. Phys. J. D **9**, 479 (1999).
[10] L. Zhang, D. Xue, and C. Gao, J. Magn. Magn. Mater. **267**, 111 (2003).
[11] M. Ghosh, E. V. Sampathkumaran, and C. N. R. Rao, Chem. Mater. **17**, 2348 (2005).
[12] A. Punnoose, H. Magnone, M. S. Seehra, and J. Bonevich, Phys. Rev. B **64**, 174420 (2001).
[13] J. Tejada and X. X. Zhang, J. Phys.: Condens. Matter **6**, 263 (1994).
[14] S. Gider, D. D. Awschalom, T. Douglas, S. Mann, and M. Chaparala, Science **268**, 77 (1995).
[15] S. A. Makhlouf, F. T. Parker, and A. E. Berkowitz, Phys. Rev. B **55**, R14 717 (1997).
[16] S.-W. Cheong, J. D. Thompson, and Z. Fisk, Phys. Rev. B **39**, 4395 (1989).
[17] R. K. Kremer, E. Sigmund, V. Hizhnyakov, F. Hentsch, A. Simon, K. A. Müller, and M. Mehring, Z. Phys. B: Condens. Matter **86**, 319 (1992).
[18] R. K. Kremer, V. Hizhnyakov, E. Sigmund, A. Simon, and K. A. Müller, Z. Phys. B: Condens. Matter **91**, 169 (1993).
[19] E. Sigmund, V. Hizhnyakov, R. K. Kremer, and A. Simon, Z. Phys. B: Condens. Matter **94**, 17 (1994).
[20] C. Panagopoulos, M. Majoros, and A. P. Petrović, Phys. Rev. B **69**, 144508 (2004).
[21] M. Majoros, C. Panagopoulos, T. Nishizaki, and H. Iwasaki, Phys. Rev. B **72**, 024528 (2005).
[22] C. Panagopoulos, M. Majoros, T. Nishizaki, and H. Iwasaki, Phys. Rev. Lett. **96**, 047002 (2006).
[23] J. M. Hill, D. C. Johnston, and L. L. Miller, Phys. Rev. B **65**, 134428 (2002).
[24] A. N. Lavrov, Y. Ando, S. Komiya, and I. Tsukada, Phys. Rev. Lett. **87**, 017007 (2001).
[25] G. Wübbeler, O. F. Schirmer, and S. Köhne, Phys. Rev. B **54**, 9054 (1996).
[26] J. Tejada, X. X. Zhang, and E. M. Chudnovsky, Phys. Rev. B **47**, 14977 (1993).
[27] V. I. Nizhankovskii, A. I. Khar'kovskii, and A. J. Zaleski, Eur. Phys. J. B **10**, 761 (1999).
[28] V. I. Nizhankovskii, J. Magn. Magn. Mater. **242-245**, 928 (2002).
[29] W. H. Meiklejohn and C. P. Bean, Phys. Rev. **105**, 904 (1957).
[30] I. Dzyaloshinsky, J. Phys. Chem. Solids **4**, 241 (1958).
[31] V. Chechersky, N. S. Kopelev, B. H. O. M. I. Larkin, J. L. Peng, J. T. Markert, R. L. Greene, and A. Nath, Phys. Rev. Lett. **70**, 3355 (1993).
[32] V. Chechersky, N. S. Kopelev, A. Nath, J.-L. Peng, R. L. Greene, B. H. O. M. I. Larkin, and J. T. Markert, Phys. Rev. B **54**, 16254 (1996).
[33] I. Watanabe, T. Uefuji, H. Kurahashi, M. Fujita, K. Yamada, and K. Nagamine, Physica C **357-360**, 212 (2001).